Structural Integrity Evaluation of Axial Outside Diameter Stress Corrosion Cracking at Supports for Arkansas Nuclear One, Unit 2, During Cycle 14 Post Mid-Cycle Operation

AES AES 99113855-1-1
March 2000

Prepared for

Entergy Operations, Inc.

APTECH
IS APPLIED TECHNOLOGY

APTECH IS APPLIED TECHNOLOGY ®

AES 99113855-1-1
March 2000

Structural Integrity Evaluation of Axial Outside Diameter Stress Corrosion Cracking at Supports for Arkansas Nuclear One, Unit 2, During Cycle 14 Post Mid-Cycle Operation

Prepared by

Brian W. Woodman
Peter S. Jackson

APTECH ENGINEERING SERVICES, INC.

Prepared for

Entergy Operations, Inc.
Route 3, Mail Box 137-G
Russellville, Arkansas 72801

Attention: Mr. Dan Meatheany

APTECH ENGINEERING SERVICES, INC.
1282 REAMWOOD AVENUE ☐ SUNNYVALE ☐ CA 94089
POST OFFICE BOX 3440 ☐ SUNNYVALE ☐ CA 94089-3440 ☐ (408) 745-7000 ☐ FAX (408) 734-0445
HOUSTON, TX ☐ (281) 558-3200 ☐ CHARLOTTE, NC ☐ (704) 865-6318
ST. LOUIS, MO ☐ (636) 394-2653 ☐ WASHINGTON, DC ☐ (301) 868-4899

© Aptech Engineering Services, Inc.

NOTICE

This report was prepared by Aptech Engineering Services, Inc., (APTECH) as an account of work sponsored by the organization named herein. Neither APTECH nor any person acting on behalf of APTECH: (a) makes any warranty, express or implied, with respect to the use of any information, apparatus, method, or process disclosed in this report or that such use may not infringe privately owned rights; or (b) assumes any liabilities with respect to the use of, or for damages resulting from the use of, any information, apparatus, method, or process disclosed in this report.

TABLE OF CONTENTS

Section **Page**

1 Introduction 1-1

2 Probabilistic Model 2-1
2.1 Introduction 2-1
2.2 General Description of the Probabilistic Model 2-2
2.3 Synthesis of Defect Depth Distribution 2-3
2.4 Incorporation of Fully Probabilistic Modeling for Growth Rate, Detection Process, and Burst 2-5

3 Structural Integrity and Leak Rate Models 3-1
3.1 Idealized Axial Crack Profiles 3-1
3.2 Axial Crack Burst Pressure Calculation 3-3
3.3 Axial Crack Leak Rate Calculation 3-3

4 Analysis Input Parameters 4-1
4.1 Tubing Mechanical Properties 4-1
4.2 Degradation Length Distribution 4-1
4.3 Modeling of Flaw Detection 4-2

5 Growth Rate Evaluation 5-1
5.1 Growth Rate of Axial Flaws at ANO U2 Eggcrates 5-1
5.2 Apparent Growth Rates at 2P99 5-1
5.3 Axial Flaw Growth Model 5-2
5.4 Axial Flaw Form Factor for Flaws Profiled at 2P99 5-3
5.5 Adjusted Growth Rate Distribution 5-4

6 RESULTS: Structural Margin and Leakage Evaluations 6-1

References R-1

Section 1
INTRODUCTION

An assessment of steam generator tubing potentially affected by outside diameter stress corrosion cracking (ODSCC) at eggcrates was conducted for Arkansas Nuclear One, Unit 2 (ANO-2) for operation between 2P99 (mid-cycle) and 2R14. This mode of degradation is of particular concern following the 2P99 eddy current inspection in which a much larger number of eggcrate flaws were found. In situ testing of the largest flaws showed leakage in two instances. In one instance, the leakage exceeded test capability near the 3ΔP level. Neither flaw exhibited measurable leakage at steam line break (SLB) conditions.

Subsequent reevaluation of prior nondestructive examination (NDE) data showed the defect in question to be detectable at prior inspections using the most recent (2P99) calling criteria. This was also true of many of the larger indications encountered in the 2P99 inspection. This outcome was unexpected due to the incorporation of an all rotating probe resolution process in the 2R13 examination which had, in fact, removed a significant additional number of defects from service.

In response to the outcome of the 2P99 inspection, a revised model was developed for use in the current analysis which relies only on the probability of detection information generated in the post-2R13 site-specific performance demonstration (SSPD) (1). Since inspection data are only available from one inspection (2P99) performed after the SSPD, a single-cycle model was selected for use in the analysis performed for the current operating period.

The single-cycle model developed for ANO-2 (2P99 – 2R14) replaces the multi-cycle model that has been used extensively by Aptech Engineering Services, Inc. (APTECH) for similar analyses in the past (2 through 6). The multi-cycle model used a Monte Carlo simulation process to follow crack initiation, detection, growth, and repair over several cycles of operation.

The single-cycle model is, in fact, very similar to the previous model in that the growth process, structural integrity, and leakage integrity are modeled in virtually identical ways. The major difference between the single-cycle and multi-cycle models is the process by which the hidden (unrepaired) population is inferred. The single-cycle model is discussed extensively in Section 2 of this report.

A description of the methods of characterizing crack shapes and critical dimensions for axial cracking is presented in the next sections of the report. This is followed by explanations of burst pressure and leak rate calculations. Next, input to the Monte Carlo simulation programs is defined, then the simulation steps are discussed. Finally, leak rate and conditional probability of burst (POB) results are presented specific to ANO-2 operation until the scheduled refueling outage at 2R14.

Section 2
PROBABILISTIC MODEL

2.1 INTRODUCTION

The probabilistic model for axial cracking at eggcrates is fundamentally similar to that used by APTECH for evaluation of structural and leakage integrity in several other plants (2 through 6). There are, however, four basic alterations to the model, one of which is specifically appropriate for the ANO-2 analysis for the remaining Cycle 14 operation. The alterations include:

- Use of a single-cycle approach to synthesize the undetected defect population
- Incorporation of a fully probabilistic capability for defect growth modeling
- Incorporation of a probabilistic capability for POD modeling
- Addition of a probabilistic capability in the structural integrity computation

The most fundamental of these changes is the use of a single-cycle model to determine the state of the steam generator in terms of defects present at the beginning of the operating period.

In prior analyses for ANO-2, APTECH used a multi-cycle model for this purpose. In the case of the multi-cycle model, the processes of initiation, growth, and inspection/repair are explicitly modeled. Information available from prior inspection results is used to benchmark the predictions at each prior inspection. The critical benchmarks involved in

the multi-cycle model include the number of defects observed, distribution of defect depths, and extreme depths. By contrast, a single-cycle model uses no prior cycle inspection information. The unrepaired (hidden) defect population present at beginning-of-cycle (BOC) is inferred directly from the measured defects present and POD considerations. In this sense, the single-cycle model is conceptually more straightforward. There is a fundamental difference between the information content in the two types of models. In the case of the single-cycle model, the inference of the hidden population is based purely on POD and, therefore, represents what could be present and undetected. In the multi-cycle model, the inference is based on further considerations, including the dynamic evolution of the defect population and, therefore, represents what is likely to be present and undetected.

The multi-cycle model predictions are sensitive to inspection transients or changes in effective POD from cycle to cycle. The unavailability of SSPD results for ANO-2 for inspections prior to 2P99 suggests that the single-cycle approach is more appropriate for the structural integrity assessment of the ANO-2 steam generators during the final Cycle 14 operating period.

2.2 GENERAL DESCRIPTION OF THE PROBABILISTIC MODEL

The probabilistic model used in the present ANO-2 analysis projects the growth of defects left behind in the most recent inspection to obtain representative sample defect populations from which structural and leakage integrity assessments can be made. These assessments are performed at end-of-cycle (EOC) conditions or, if necessary, at other times during the plant operating period of interest. Specifically, Monte Carlo simulation of the processes of eddy current inspection, crack growth, tube rupture, and crack leakage under postulated accident conditions are used to estimate the probability of tube burst and magnitude of leakage. The Monte Carlo simulation for the ANO-2 analysis utilized 1 million trials.

The state of degradation of the steam generator tubing is simulated in the model by a defect population that is defined by several attributes. These attributes include the population size and the distributions of length, structural depth, peak depth, and material properties. Given a randomized set of these attributes for each defect in the simulated population, an estimate of burst pressure and leakage can be made for each member of the defect population. From these estimates, population attributes, such as total leakage and minimum burst pressure may be obtained. The general flow for this process, which constitutes a single Monte Carlo trial, is shown in Figure 2-1.

The overall simulation process consists of many thousands of individual Monte Carlo trials, each of which simulates the defect state of a complete steam generator for a given degradation mechanism. The simulation process generates a record of the results of all trials performed from which overall burst and leakage probabilities may be inferred and appropriate distributional information obtained. Other pertinent data from each trial, such as material properties, flaw length, and crack shape factors for minimum burst pressure (worst) defects, are also recorded.

2.3 SYNTHESIS OF DEFECT DEPTH DISTRIBUTION

The EOC defect depth population is obtained in the single-cycle model for a BOC depth population convoluted with a randomized growth rate for each defect in the population. In the case of structural integrity, the structural average depth (see Section 3 of this report) is the characterizing variable. The details of the inference of growth rate distributional characteristics is discussed in Section 5. The relationship between structural depth and peak depth, which is the characterizing variable for leakage and detection considerations, is discussed in Section 4.

The elements of the EOC defect population are given by:

$$[D_{ST}(EOC)]_i = [D_{ST}(BOC)]_i + [G_{ST}]_i \Delta T$$

where,

$[D_{ST}(EOC)]_i$ = Structural average depth at EOC, iTh defect

$[D_{ST}(BOC)]_i$ = Structural average depth at BOC, iTh defect

$[G_{ST}]_i$ = Randomized growth rate

ΔT = Operating interval

The BOC defect population is inferred directly from the measured defects in the most recent inspection. Each measured defect has an associated POD and, therefore, a probability that a similar defect exists and remains undetected and in service for the upcoming period of operation. In the case of a typical rising rate POD function the deeper observed defects have a relatively low probability of hidden corresponding defects. The less deep defects have a higher likelihood of one or more corresponding defects. The general inference process for a given Monte Carlo trial is shown in Figure 2-2. For each observed defect, a corresponding POD is computed. Using the POD for that defect, a set of randomized trials are performed to determine the number of attempts required to detect the defect. The number of hidden corresponding defects is simply the number of attempts minus 1 for the defect actually found. This process is repeated for all measured defects. The BOC defect population is the total of all of the corresponding hidden defects. Since these defects are expressed in terms of peak depth, a randomized set of form factors, as discussed in Section 4, are used to obtain the population of BOC structural average depths.

2.4 INCORPORATION OF FULLY PROBABILISTIC MODELING FOR GROWTH RATE, DETECTION PROCESS, AND BURST

In prior probabilistic models the probability distribution representing the defect growth process was limited to a single parameter set. With the development of the new growth rate inference methodology described in Section 5 of this report, a fully probabilistic implementation of the defect growth methodology was incorporated into the model. The current model samples from a set of 1,000 growth rate distributions to obtain the parameter set for a given Monte Carlo trial.

The recent work involving the post-2R13 SSPD at ANO-2 (1) has indicated a need for more diversified modeling of the detection process on a team-specific basis. This capability to model selection of a randomized team has been incorporated in the current model. In the present implementation, the five teams represented in the ANO-2 SSPD are selected at random in the simulation.

The burst pressure computation for a given defect used a lower limit relationship for part-through-wall defects in prior analyses. When compared with actual pulled-tube data, this approach leads to an average conservatism of more than 1000 psid in burst pressure. The present model has the ability to utilize an additive error component, which regains significant burst margin and permits more realistic estimation of POB. The error component is Beta distributed with a minimum value of –163 psid and an average value of 1080 psid. The maximum error is approximately 3000 psid.

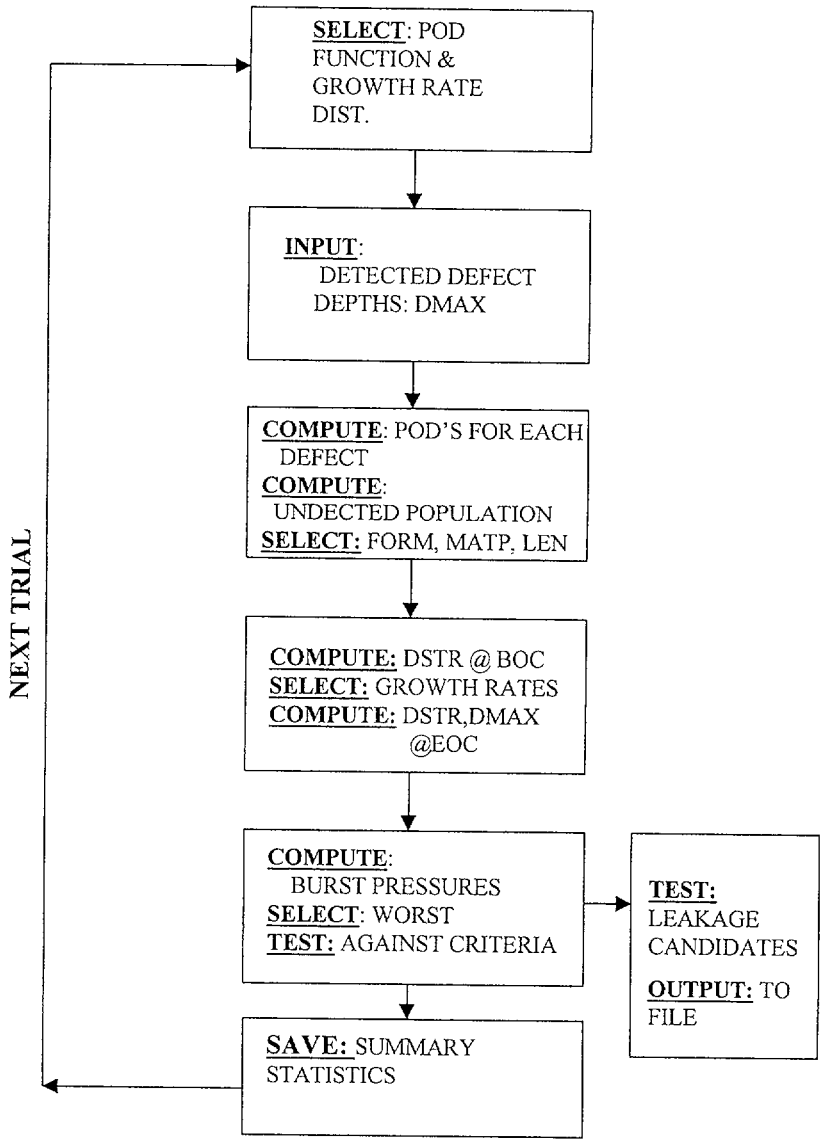

Figure 2-1 — Algorithm for Individual Monte Carlo Trial.

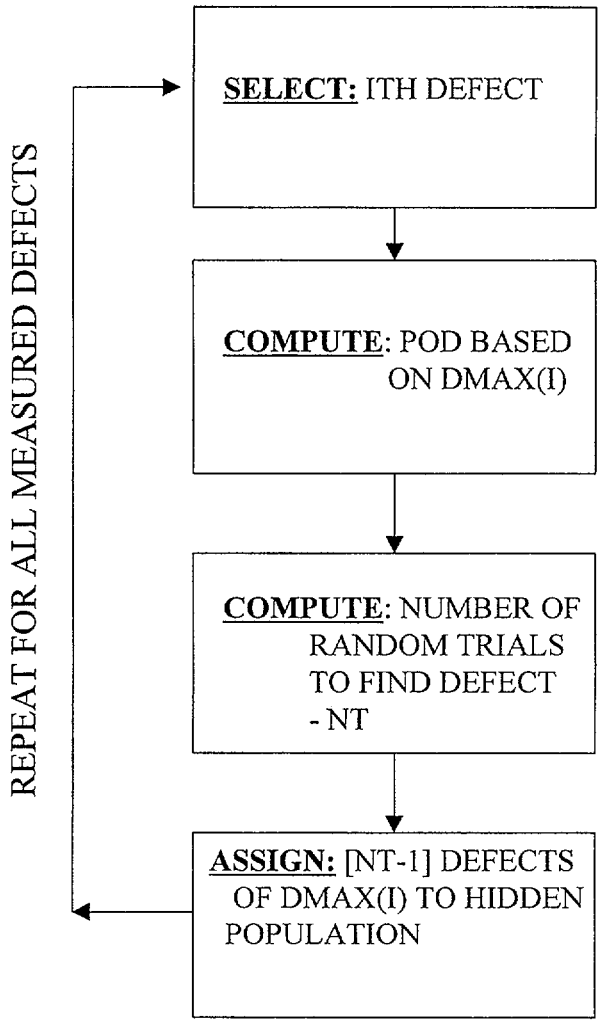

Figure 2-2 — Construction of Undetected Population for Simulation.

Section 3
STRUCTURAL INTEGRITY AND LEAK RATE MODELS

Burst strength and leak rate calculations for tubes exhibiting axial corrosion degradation are based on idealized crack profiles. Axial degradation is modeled as planar cracking. Given that examination of pulled tubes from ANO-2 has revealed some components of intergranular attack (IGA) and multiple crack planes, the planar crack assumption is conservative in both burst and leak rate calculations. The following paragraphs describe idealized morphologies for axial cracks and corresponding burst and leak rate equations.

3.1 IDEALIZED AXIAL CRACK PROFILES

From the perspective of tube burst strength and leak rate calculations, each axial corrosion indication is idealized as a single planar crack. This is conservative in that the strengthening and leak limiting effects of ligaments between crack segments in physical crack arrays are neglected. In addition, the physical depth profile, which typically varies in a nonuniform fashion over the length of the crack, is modeled as a simplified ideal profile for burst and leak calculations.

Figure 3-1 illustrates the idealized crack profiles used for burst and leak calculations compared to the corresponding physical depth profile as measured during a pulled-tube destructive examination. The idealized burst profile represents the portion of the physical profile that is structurally significant in computing burst pressure. The structurally significant dimensions are determined using the Structural Minimum Method (2 through 6), as follows. The physical profile is discretized over its length using a reasonable

number of segments, typically between 20 and 50. For each contiguous portion of the crack (that is, for each potential structurally significant length segment), a corresponding depth is computed by equating the areas under the physical and ideal profiles. Each length and depth pair is then tested using the Framatome burst equation (7) (described below) to find the dimensions that minimize the computed burst pressure. The length and depth that minimize the burst pressure represent the structurally significant dimensions and, hence, define the idealized burst profile. It is essential to note that historical measurements have shown the structurally significant length of a crack to be essentially equal to the portion of a physical crack length detected by a rotating pancake coil (RPC) eddy current probe (2).

The idealized leak profile length is identical to the structurally significant length computed for the burst profile. The tent-shaped leak profile is then determined by equating the maximum depth penetration for both physical and ideal profiles, and by again balancing the areas under the respective profiles over the structural length. The profile form factor, F, is defined to be the ratio of the maximum depth, d_{max}, to the structurally significant depth, d_{st}. The distribution characteristics of this form factor are based on pulled tube destructive examination data (8), as shown in Figure 3-2.

Crack growth over time is assumed to occur primarily in the depth direction. The structural length for both burst and leak profiles is considered to be constant in time. For leakage calculations, the form factor is assumed to remain constant as the crack propagates through-wall (TW), as shown in Figure 3-3. The profile dimension, d_s, is related to the structurally significant depth as $d_s = 2d_{st} - d_{max}$. The length of the TW segment, L_{leak}, is then defined by the geometry of the idealized profile to be:

$$L_{leak} = L_{st} \frac{d_{st} F - t}{2d_{st} (F - 1)}$$

3.2 AXIAL CRACK BURST PRESSURE CALCULATION

Given the structurally significant length and depth dimensions as computed above, the burst pressure for an axially degraded tube is computed via the Framatome partial TW burst equation:

$$P = \frac{0.58St}{R_i}\left[1 - \frac{Ld/t}{L + 2t}\right]$$

where P is the estimated burst pressure, S the sum of the yield and ultimate tensile strengths of the tube material, t the tube thickness, R_i the inner radius of the tube, L the characteristic degradation length, and d the characteristic degradation depth. The Framatome equation, when used with the structurally significant dimensions (L_{st} and d_{st}), produces consistently conservative burst pressure estimates compared to measured burst data, as shown in Figure 3-4. It is an excellent lower bound to an extensive set of pulled-tube burst test data. A fully detailed description of the APTECH burst pressure methodology is given in Ref. 15.

3.3 AXIAL CRACK LEAK RATE CALCULATION

As described in Ref. 9, Version 3.0 of the PICEP two-phase flow algorithm was used to compute flow rates through cracks as a function of pressure differential (p), temperature (T), crack opening area (A), and total TW crack length (L). Friction effects and crack surface roughness were included in the model. SLB, room temperature, and normal operating condition leak rates calculated by PICEP were fitted to regression equations. The PICEP-based leak rate regression equation for SLB conditions is given as:

$$Q = \{a + b \exp[c(A/L)^{0.451} + d(A/L)]\} Ap^{1.333}$$

where a through d are regression coefficients, as determined by an analysis of PICEP results. The leak rate Q is expressed in terms of gallons per minute at room temperature (70°F). To convert to gallons per minute at any other temperature, the calculated Q is multiplied by the ratio of the specific volume of water at temperature (T) to the specific volume of water at 70°F. The pressure, p, is in units of psi, A is in inches^2 and L (equivalently L_{leak}, as defined above) is in inches. The crack opening area is calculated using a twice-iterative plastic zone correction to adjust the linear elastic solution for plasticity effects. Further details of the PICEP regression equations and the crack opening area derivation can be found in Refs. 10 and 11.

A check of the validity of the leak rate equations is provided by a comparison of calculated leak rates versus measured leak rates listed in Ref. 12. Measured leak rates at typical normal operating steam generator conditions are available for axial fatigue cracks in steam generator tubing and axial stress corrosion cracks in steam generator tubing. Leak rates through stress corrosion cracks are less than those through-fatigue cracks of the same length because of the more torturous cracking in stress corrosion samples. A good conservative leak rate calculation methodology is considered to be one which is a closer match to leak rate results from fatigue cracks rather than stress corrosion cracks. Figure 3-5 shows that this criterion is met by the chosen methodology. Calculated leak rates, illustrated by the dotted lines in Figure 3-5, serve as a good bound to data from stress corrosion cracked samples of the same tubing dimensions. The calculated leak rates are just below the measured data for fatigue cracked samples.

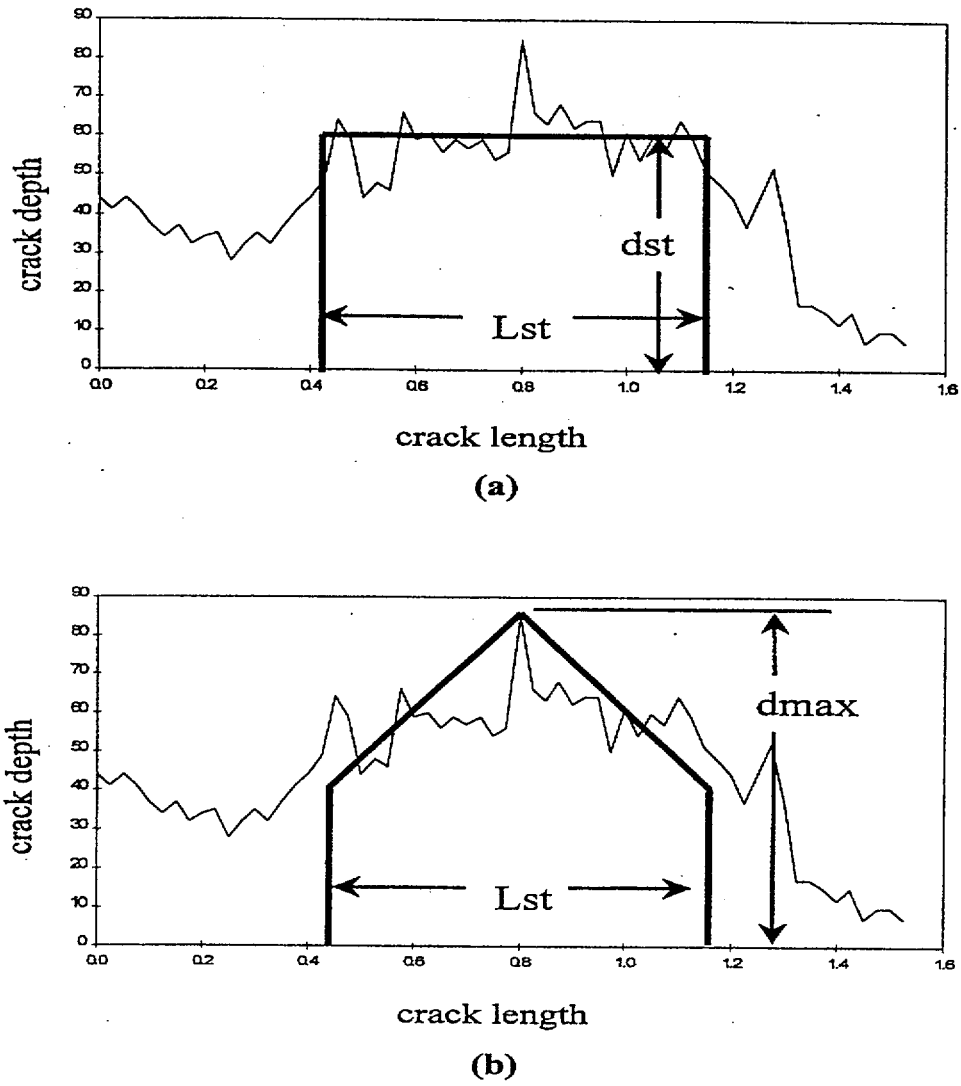

Figure 3-1 — Idealized Crack Profiles for (a) Burst and (b) Leakage.

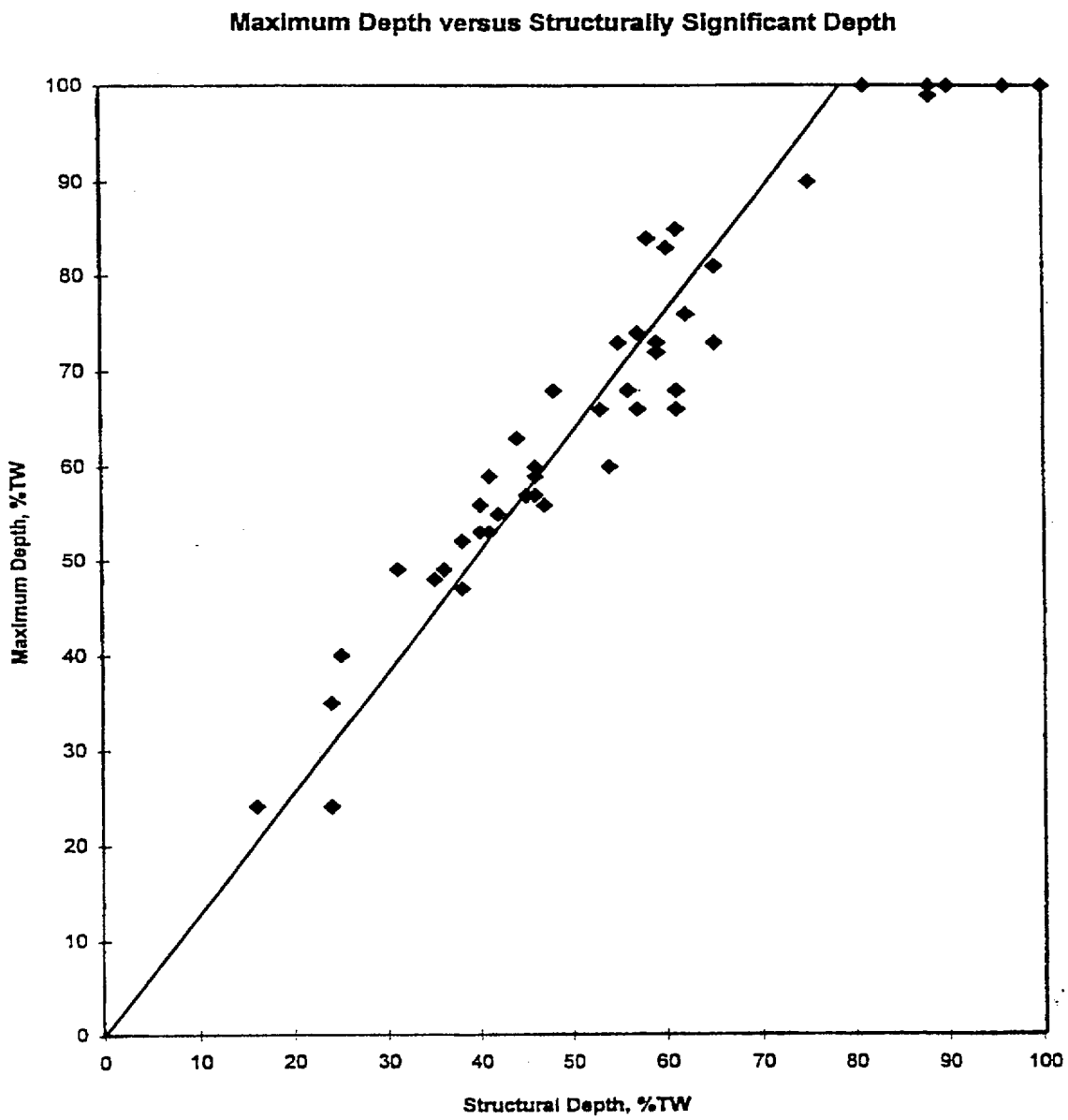

Figure 3-2 — Maximum Depth vs. Structurally Significant Depth, Pulled-Tube Data.

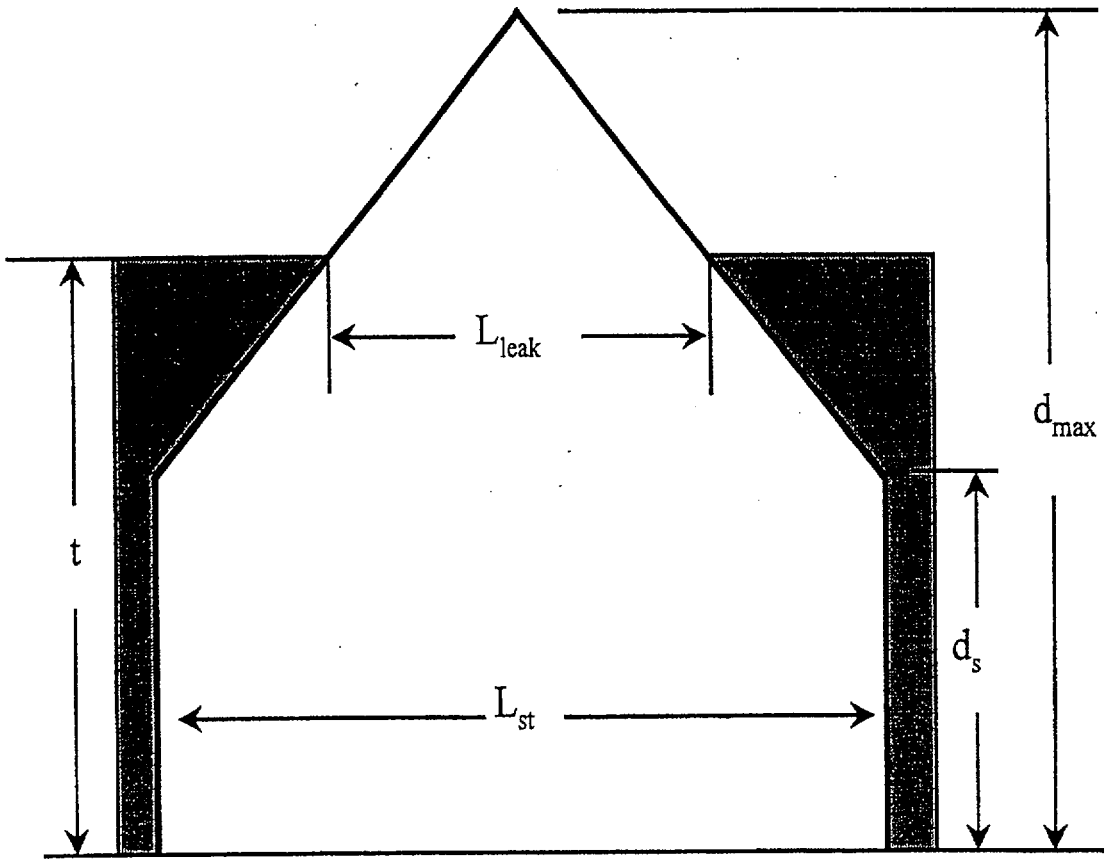

Figure 3-3 — Idealized Leakage Crack Profile After Through-Wall Penetration.

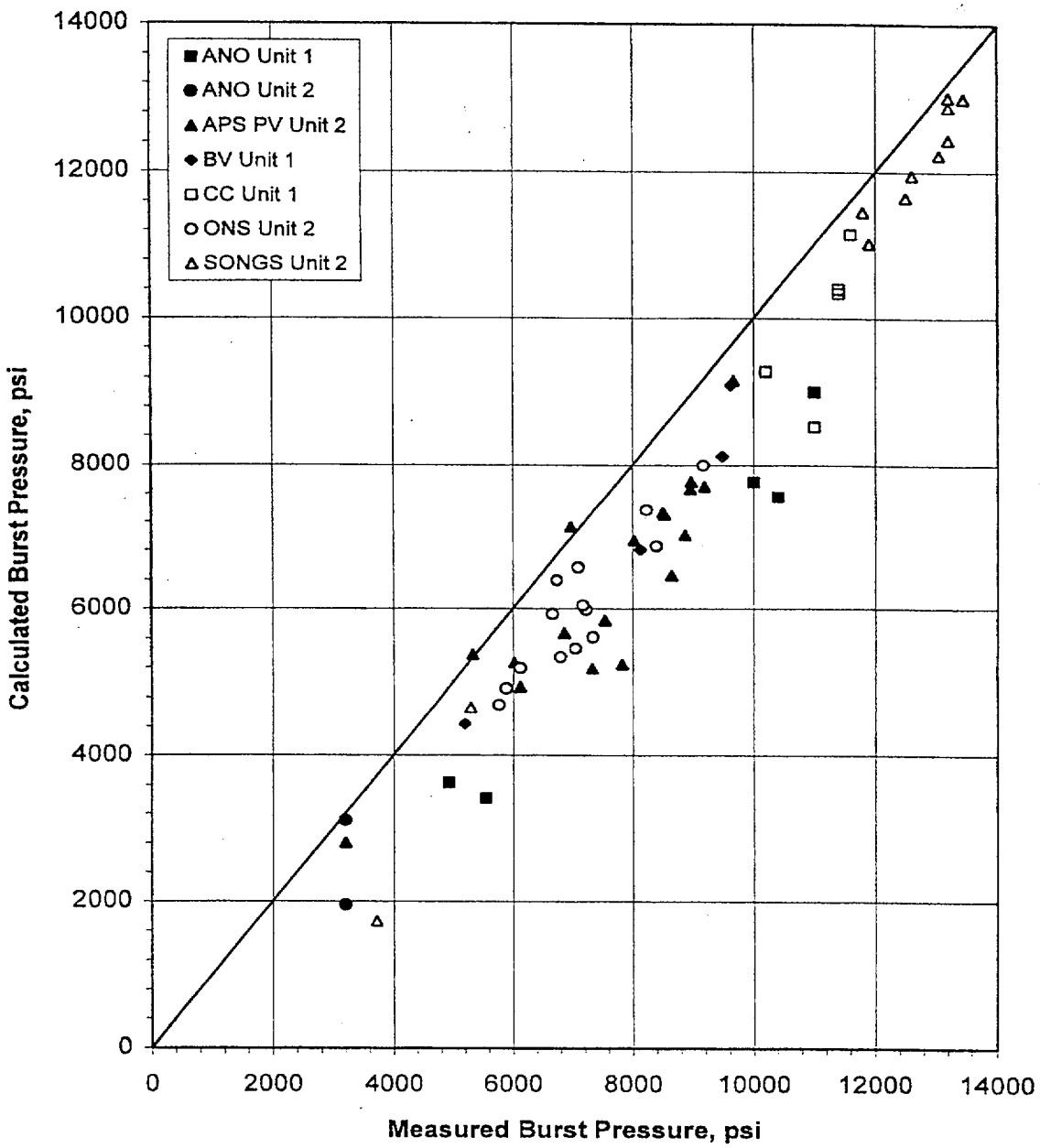

Figure 3-4 — Calculated vs. Measured Burst Pressure Using the Structural Minimum Method and the Framatome Burst Equation.

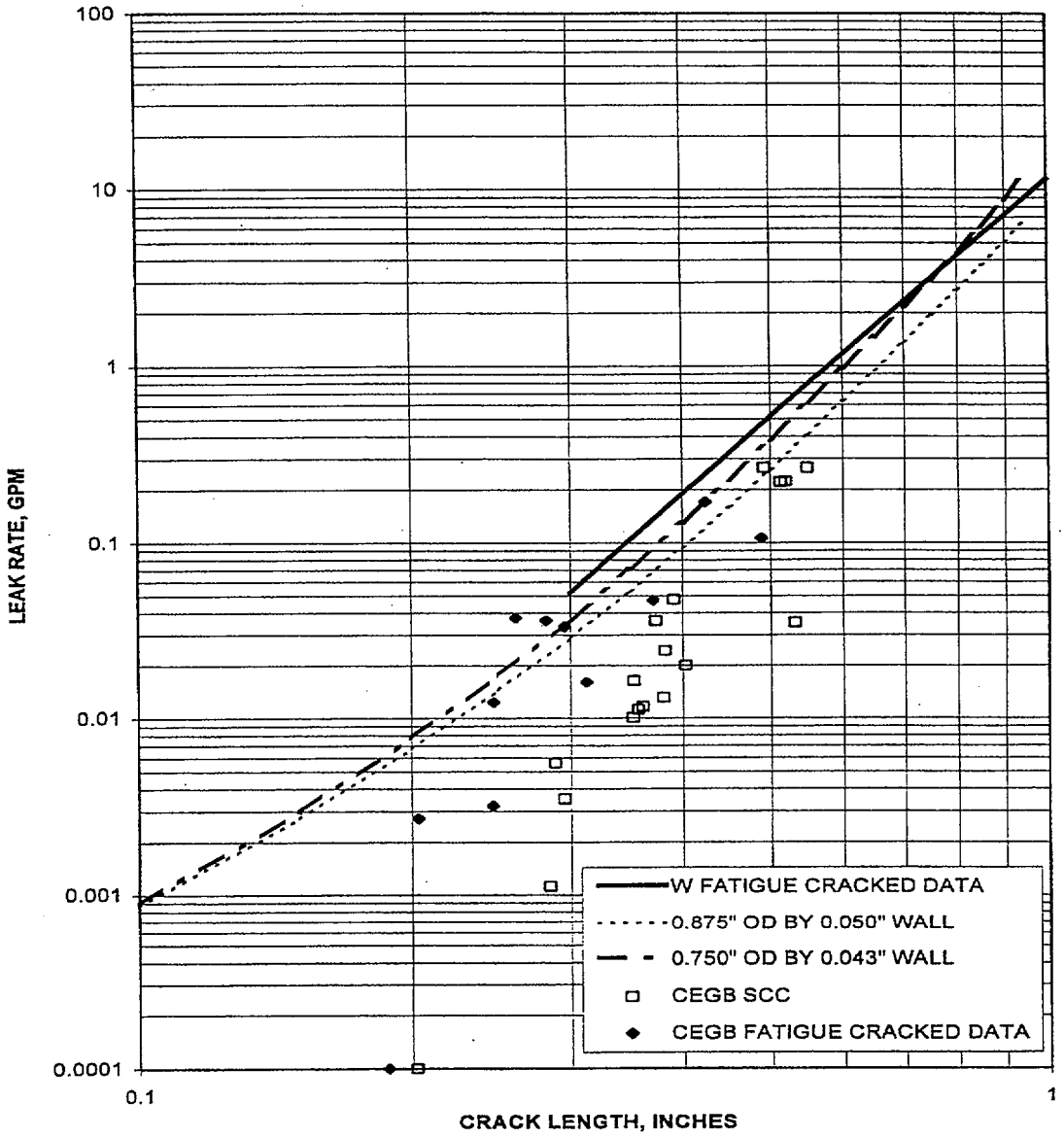

Figure 3-5 — Calculated and Measured Leak Rates for Axial Cracks in Alloy 600 Tubing at Normal Operating Conditions.

Section 4
ANALYSIS INPUT PARAMETERS

A number of input parameters are needed for the Monte Carlo simulation model. A range of material properties is considered rather than a lower bound strength value. Hence, the distribution of tensile properties of the steam generator tubing is needed. The distribution of structurally significant axial crack lengths is equated to the distribution of measured lengths as found by the RPC eddy current probe. Thus, a sampling distribution of axial crack lengths is needed. The simulation model conducts virtual inspections. This requires knowledge of the POD of degradation as a function of degradation severity for the various eddy current probes that are used. Since degradation growth is simulated, distributions of crack growth rates for axial degradation is required.

4.1 TUBING MECHANICAL PROPERTIES

Figure 4-1 shows a histogram of tube strength for both steam generators at ANO-2. The sum of yield and ultimate tensile strengths is inferred from mill reports. An adjustment has been made to correct for operating temperature. A normal distribution was fitted to the data of Figure 4-1 for application in the simulation model. This distribution was truncated at the measured extremes of the tensile property database.

4.2 DEGRADATION LENGTH DISTRIBUTION

During the eddy current inspection at the 2P99 outage, axial crack lengths were measured at eggcrate intersections near the top of the tubesheet and at freespan locations. The

distribution of lengths, as measured by the RPC probe, at eggcrate intersections in Steam Generator B is a good representative distribution and was used as the axial crack length sampling distribution in the simulation model. Figure 4-2 shows the cumulative fraction of observations versus the axial crack length. This is essentially the cumulative distribution function of the axial crack length population.

4.3 MODELING OF FLAW DETECTION

The detection capability of eddy current probes is recognized as one of the two most important factors in the outcome of tube integrity simulation studies. In the past, emphasis has been placed on characterizing the POD functions for specific probes. The recent experience at ANO-2 (2P99 inspection) has shown the importance of dealing with the NDE human factor components in a more sophisticated manner. To address this issue, a thorough study was performed (1) to evaluate the diversity of flaw detection performance for analysts representing all portions of the current NDE practice.

The present procedure for steam generation NDE evaluation utilizes multiple teams of analysts. Each team consists of a primary analyst, a secondary analyst, and a resolution team consisting of two experienced NDE analysts. If neither the primary nor secondary analyst detects the defect, the defect is undetected. If either or both detect the defect, the resolution team is called on to determine if the defect is considered real and is plugged. In the case of bobbin indications at Supports 01H – 03H, a supplementary rotating probe inspection is performed.

For the current analysis, the POD functions used were obtained directly from Ref. 1 for the most conservative data set (C′ in Table 3-4 of Ref. 1). This particular set contains the lower voltage data particularly appropriate for the ANO-2 2P99 data. An additional component of conservatism was the usage of data obtained from the bobbin resolution process rather

than using a process simulation involving rotating probe resolution. The POD functions used in the analysis to represent specific teams are shown in Figure 4-3.

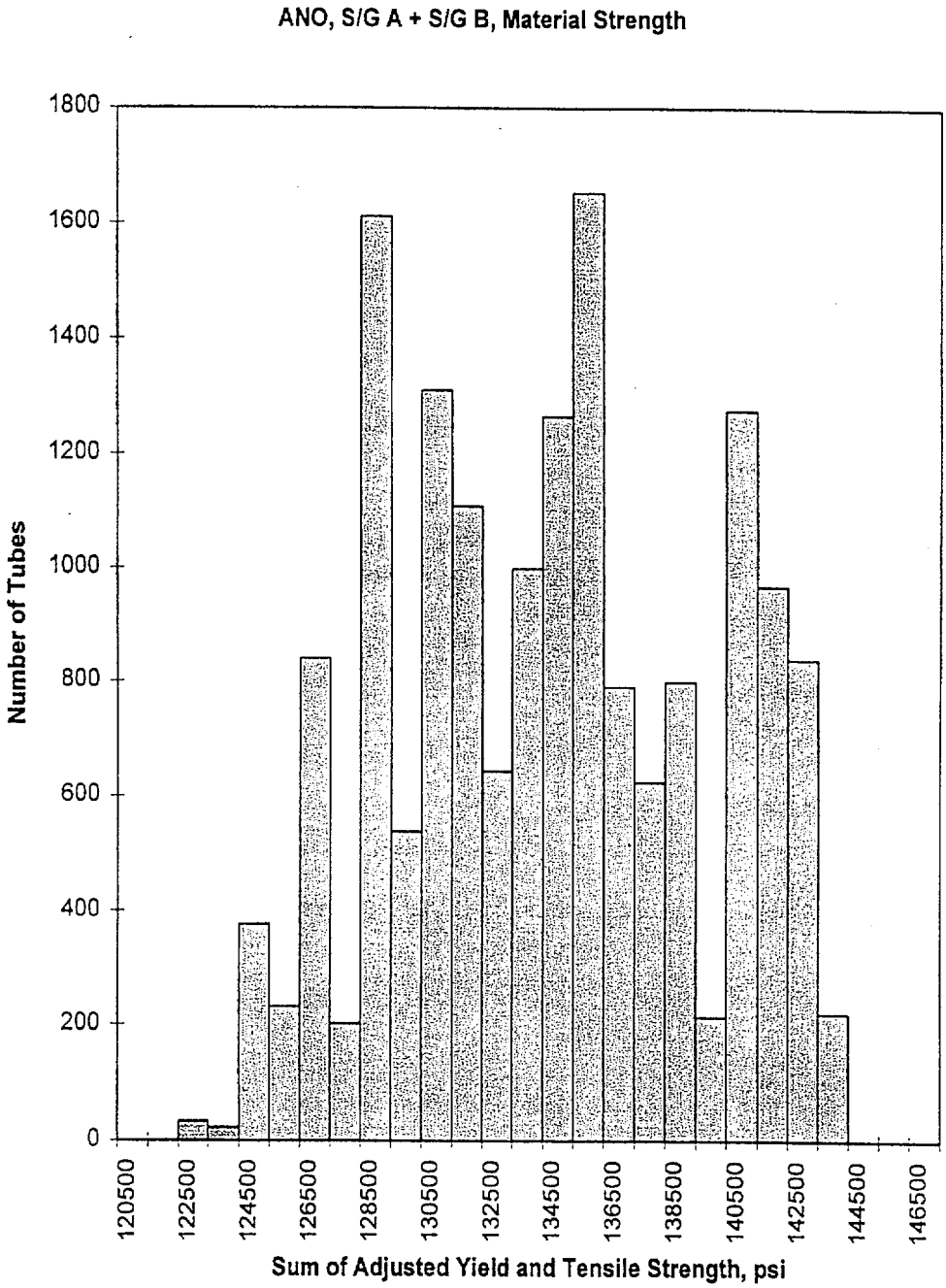

Figure 4-1 — Histogram of Tube Strength Data for ANO-2, Total for Both Steam Generators.

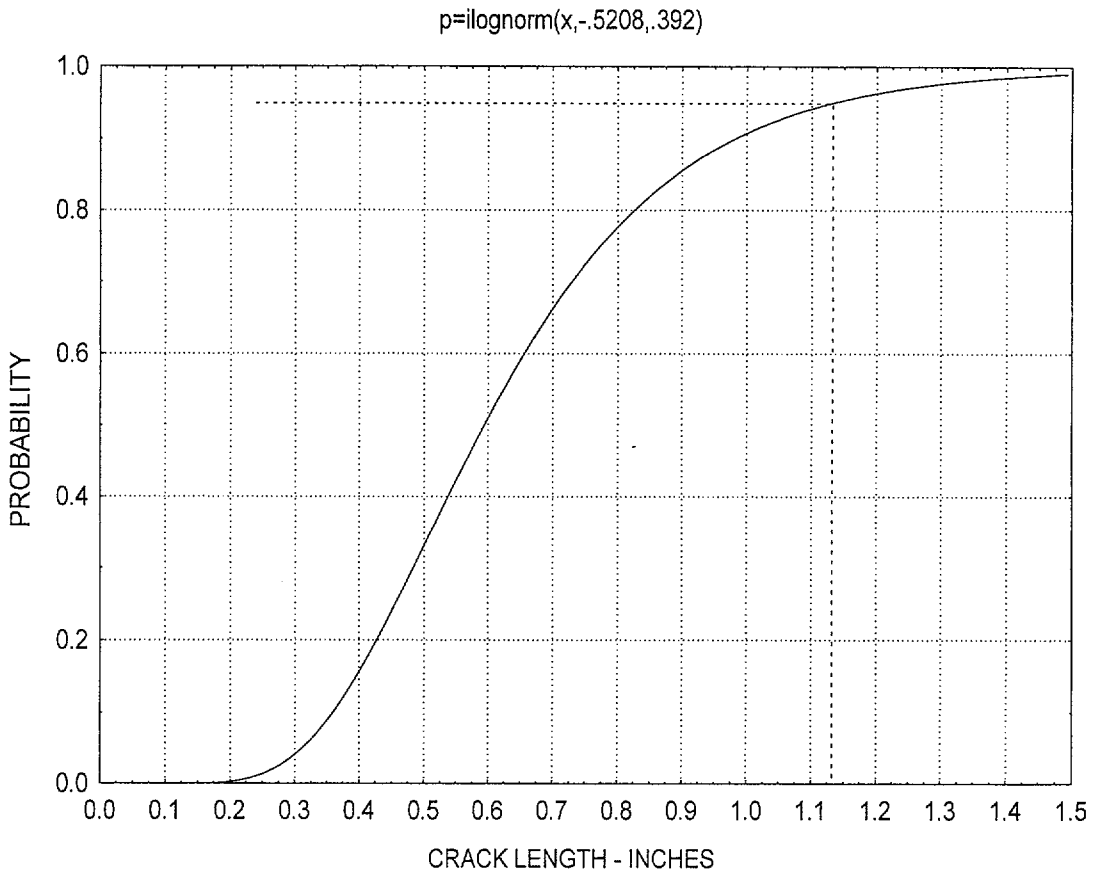

Figure 4-2 — Distribution of Axial Crack Lengths Used in Probabilistic Analysis.

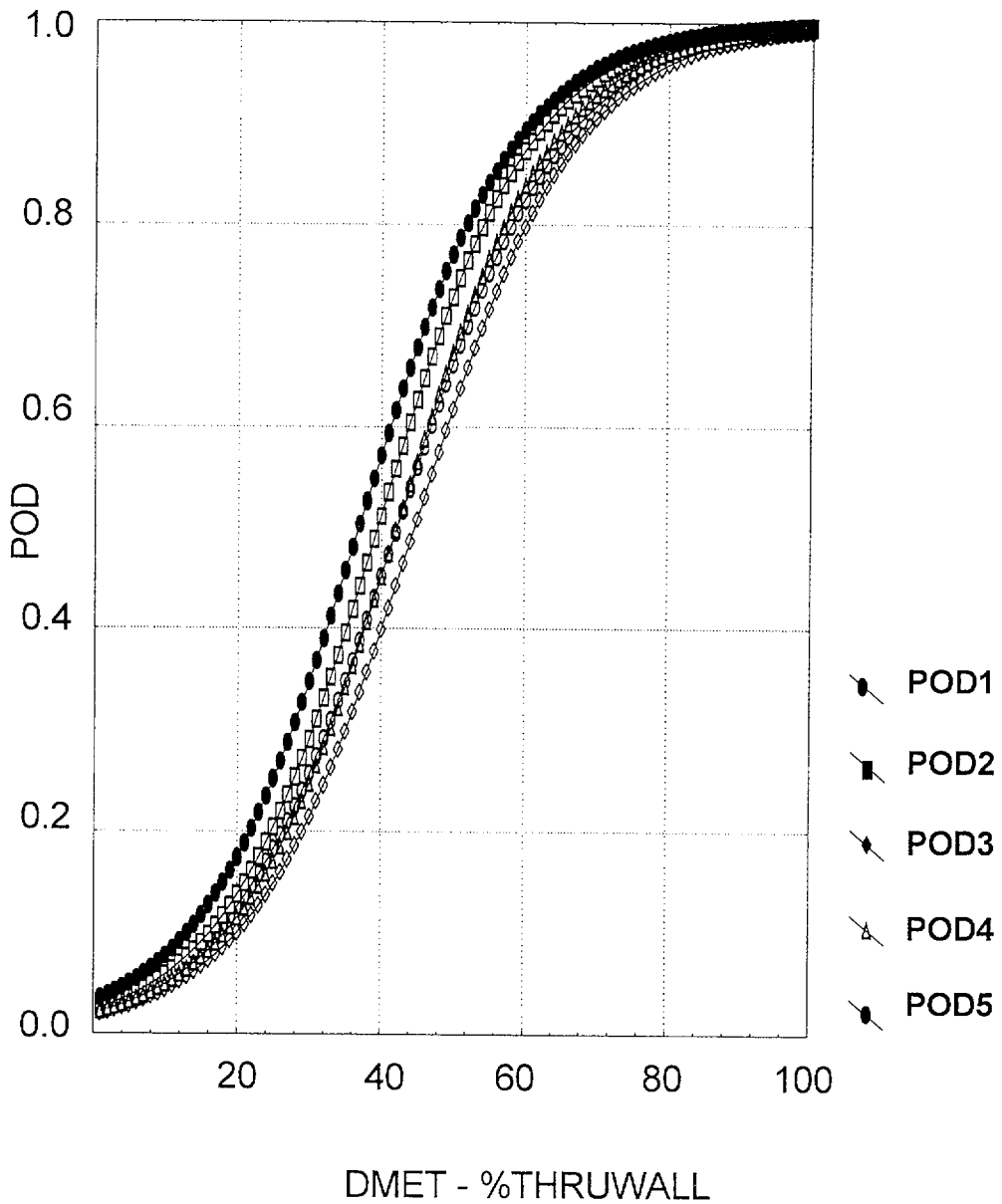

Figure 4-3 — POD Function Sets Used in Analysis.

Section 5
GROWTH RATE EVALUATION

5.1 GROWTH RATE OF AXIAL FLAWS AT ANO-2 EGGCRATES

Significant efforts have been applied over the years to determine the extent to which detected flaws in the ANO-2 steam generator tubes have changed from cycle to cycle. After the 2R12 steam generator (SG) examination, an extensive study was conducted using several Level III/QDAs. At that time, a total of 449 indications were identified for comparison, 175 from SG "A" and 274 from SG "B". This effort was performed using flaw sizes based on bobbin depth calls from the (earlier) 2F96 and 2R11 inspections. These data were then compared with the depths called at 2R12 in 1996. Figures 5-1 and 5-2 are taken from that previous axial flaw growth rate study.

At 2R12, the data from the bobbin 400/100 mix presented in Figures 5-1 and 5-2 were used to develop a lognormal statistical model of axial flaw growth. At the time, these were the only available data on which to base an axial flaw growth model for ANO-2. Data from that study were used for several cycles to justify the axial flaw growth model. The large frequency of "0" values in these figures is attributed to the convention of treating all negative apparent growth values as zero.

5.2 APPARENT GROWTH RATES AT 2P99

Figure 5-3 provides the axial flaw growth data from 2P99; the most recent inspection of the ANO-2 SG tubes. These growth data were obtained by comparing bobbin depth calls from 2P99 with depths determined from bobbin data from 2P98 and 2R13. Bobbin data were

used for the growth model because RPC data were not available for flaws detected at 2P99 (otherwise, they would have been plugged upon prior detection). A comparison of bobbin phase angle vs. met depth and RPC depth vs. met depth for available pulled-tube data sets indicates that the bobbin correlation is nearly as good as that of RPC.

While the latest growth data in Figure 5-3 are generally similar to earlier growth data, the frequency of larger growth rates (>60%/effective full power year (EFPY)) is greater. A somewhat different depiction of the ANO-2 growth data from 2P99 is presented as Figure 5-4 where negative growth values are explicitly indicated. Bobbin data from both SG "A" and SG "B" are included in Figures 5-3 and 5-4.

Figure 5-4 is normalized to the 1.48 EFPY of operation from 2P98 to the most recent inspection at 2P99. These data suggest the presence of a significant NDE uncertainty component. That is, the overall shape of the distribution, it's symmetry about a small growth value near zero, and the preponderance of negative values all are consistent with a measurement process where NDE uncertainty is the dominant statistical component for the bulk of the distribution. The empirical data, therefore, suggest that apparent growth is the superposition of an NDE uncertainty distribution and a "true" depth growth distribution.

5.3 AXIAL FLAW GROWTH MODEL

From these observations, an axial flaw growth model for the remainder of 2R14 was developed by explicitly accounting for contributions from NDE uncertainty and actual growth. The general form of the model for an observation of growth in terms of maximum depth, D_{max}, is a linear combination of normal and lognormal components for the NDE and actual growth which form the iTh observation is expressed as:

$$D_i = \delta_i + \varepsilon_i$$

$$\varepsilon_i \leftarrow N[0, \sigma_{NDE}]$$

$$\delta_i \leftarrow LN[\mu_G, \sigma_G]$$

A numerical optimization algorithm was used to determine parameters for ANO-2 axial flaw growth for the remainder of Cycle 14. The algorithm yields a super-set of families of likely parameter pairs for the actual growth component. The algorithm is constrained so as to incorporate an NDE uncertainty component that is consistent with known inspection technique uncertainties. The resulting axial flaw growth parameter super-set is indicated in Figure 5-5.

The expected correlation between the lognormal parameters is evident from Figure 5-5. Each parameter set is based on approximately 1,000 iterations of the numerical optimization algorithm. The approximate number of iterations required to obtain stable parameter set results is highly dependent on the precise formulation of the numerical optimization problem. The specific combination of inner and outer iterations that provides numerical stability was determined empirically.

The ANO-2 axial flaw growth model is an important input to the POB calculation. The family of lognormal models determined by numerical optimization accounts for uncertainties in the relative contribution to the observed (apparent) growth data from NDE uncertainty and actual growth. A large number of Monte Carlo trials are used to synthesize the growth rate distribution from the lognormal parameter sets. The equivalent distribution of actual growth rates that corresponds to this model is provided in Figure 5-6. Figure 5-6 is a "quantile" graph; it depicts the values of specific percentiles of the growth rate distribution. From this graph, the median growth rate is about 5% TW/EFPY, while the 95% value is about 17% TW/EFPY. These are point estimates (best estimates); corresponding graphs of 95/95 values are provided for comparison in Figure 5-7. Both Figures 5-6 and 5-7 are based on maximum depth. They have not been adjusted for the

form factor. The form factor accounts for the shape of the crack profile in terms of the ratio of the maximum to structural average depth.

5.4 AXIAL FLAW FORM FACTOR FOR FLAWS PROFILED AT 2P99

The computer software PROFILER was used to generate flaw profiles for more than 20 of the axial flaws detected at 2P99. The raw eddy current data were preprocessed in the course of establishing the flaw profile to limit the extent of the flaw length. PROFILER was then used to calculate the structurally significant depth of the portion of the flaws that were profiled.

These analyses were used to determine a flaw form factor, specific to ANO-2, for the remainder of Cycle 14 that accounts for the ratio between maximum depth and structurally significant flaw depth:

$$f = \frac{D_{max}}{D_{st}}$$

The flaw shape factor is, by its very nature, a statistical quantity. This variable is treated as a Gaussian random variable:

$$f \leftarrow N[\mu_f, \sigma_f]$$

Figure 5-8 provides the form factor uncertainty model that was derived from these data.

5.5 ADJUSTED GROWTH RATE DISTRIBUTION

The form factor distribution was combined with the (unadjusted) ANO-2 axial flaw growth rate distribution via a Monte Carlo procedure. The adjusted distribution that results is the

probability distribution of structurally significant depth growth rate. Figure 5-9 gives the best estimate of the flaw growth rate, adjusted for form factor. The corresponding 95% confidence limits on these quantiles are provided in Figure 5-10.

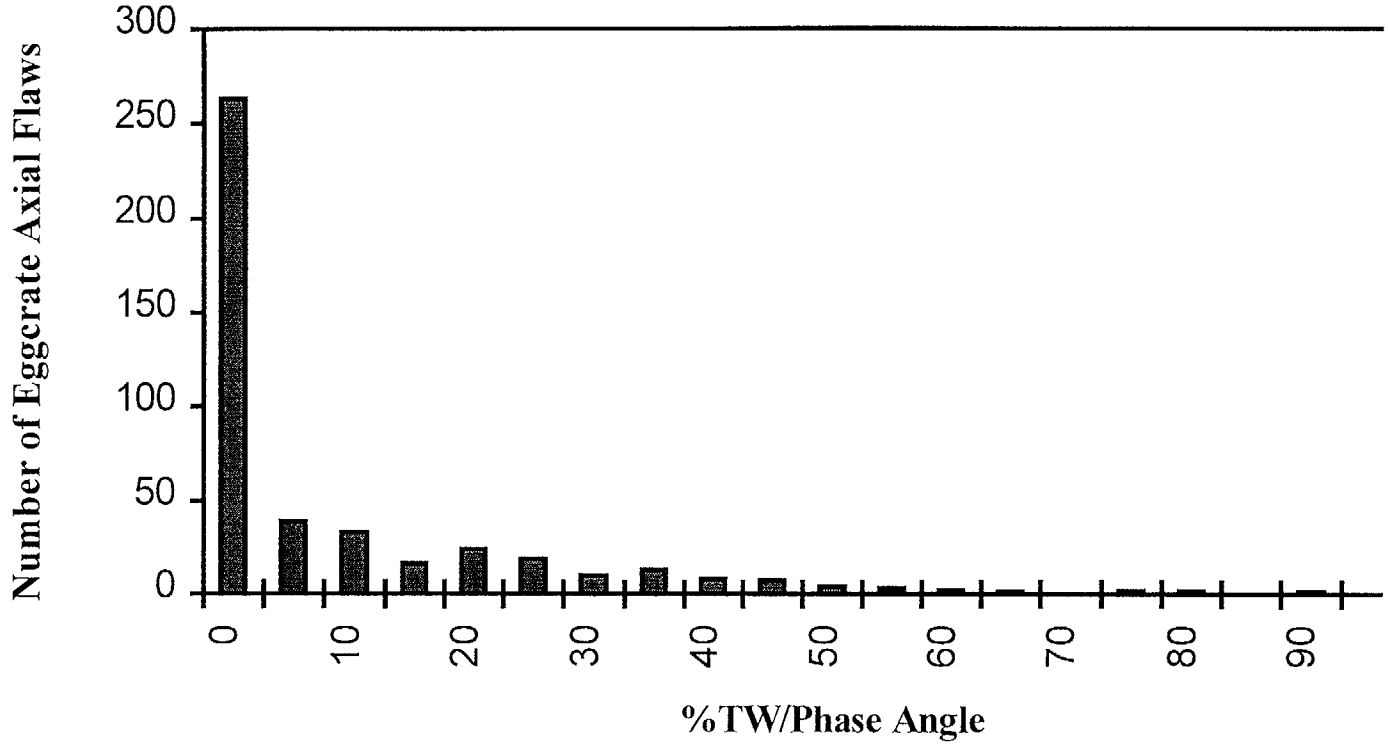

Figure 5-1 — ANO-2 Axial Flaw Growth Based on Bobbin (2R11 – 2F96).

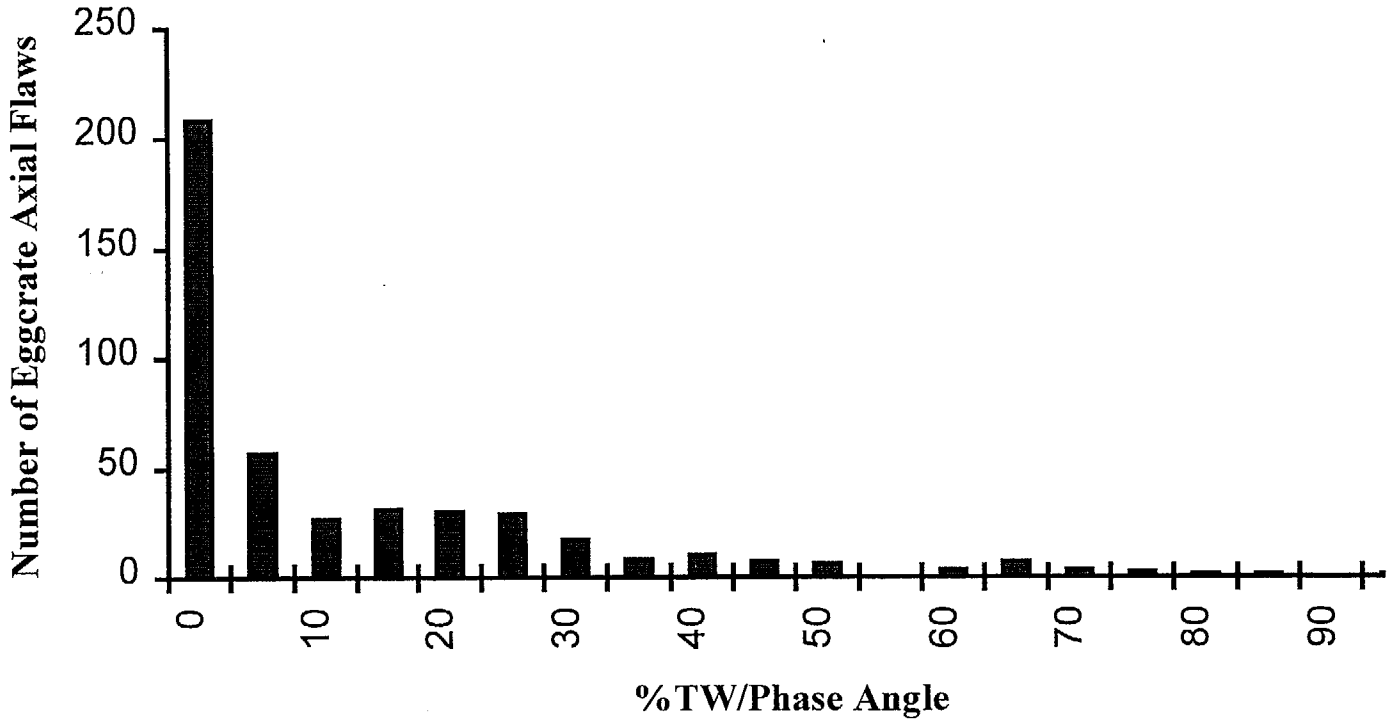

Figure 5-2 — ANO-2 Axial Flaw Growth Based on Bobbin (2R12 – 2F96).

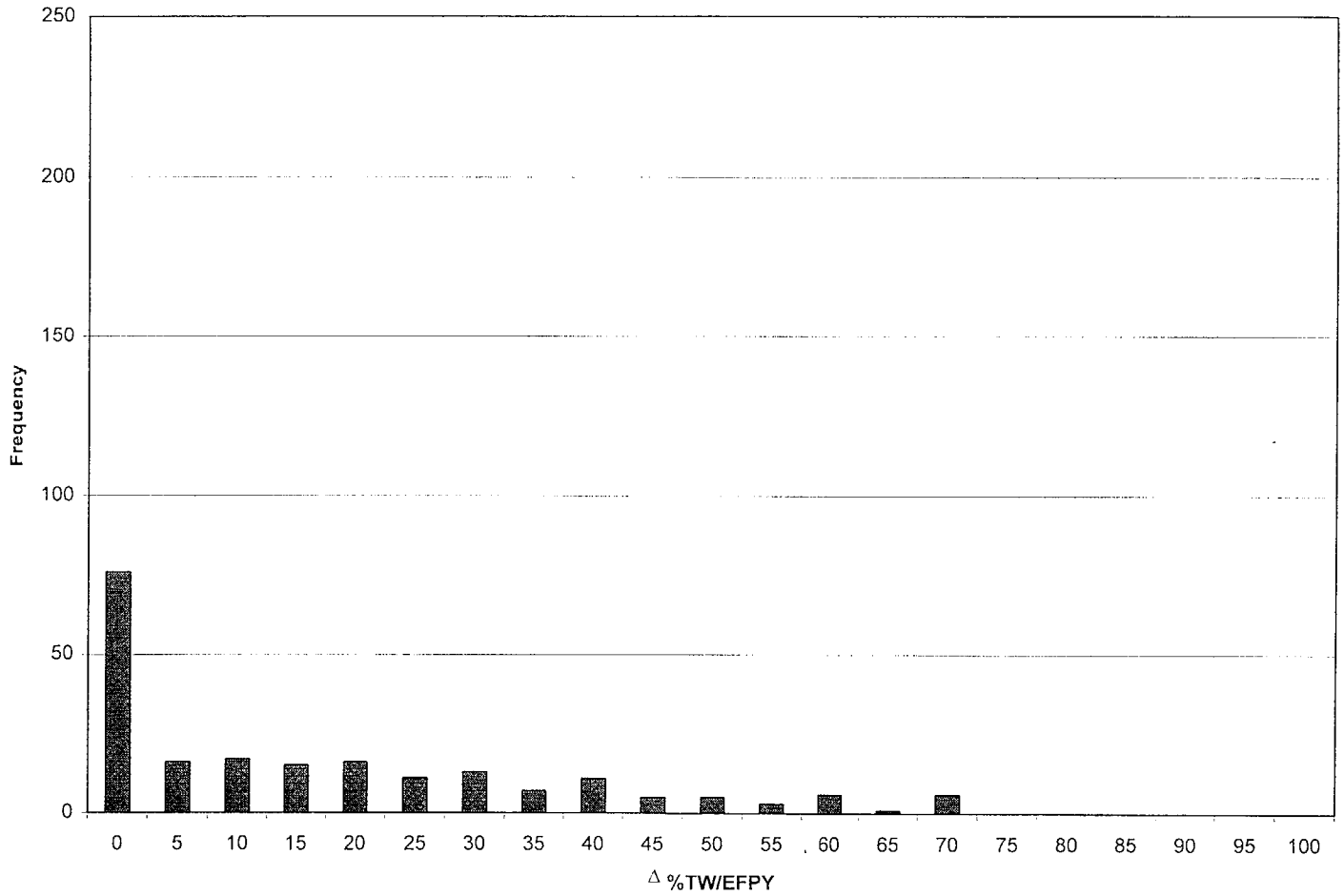

Figure 5-3 — ANO-2 Axial Flaw Growth Rate Based on Bobbin (2P99 – 2P98).

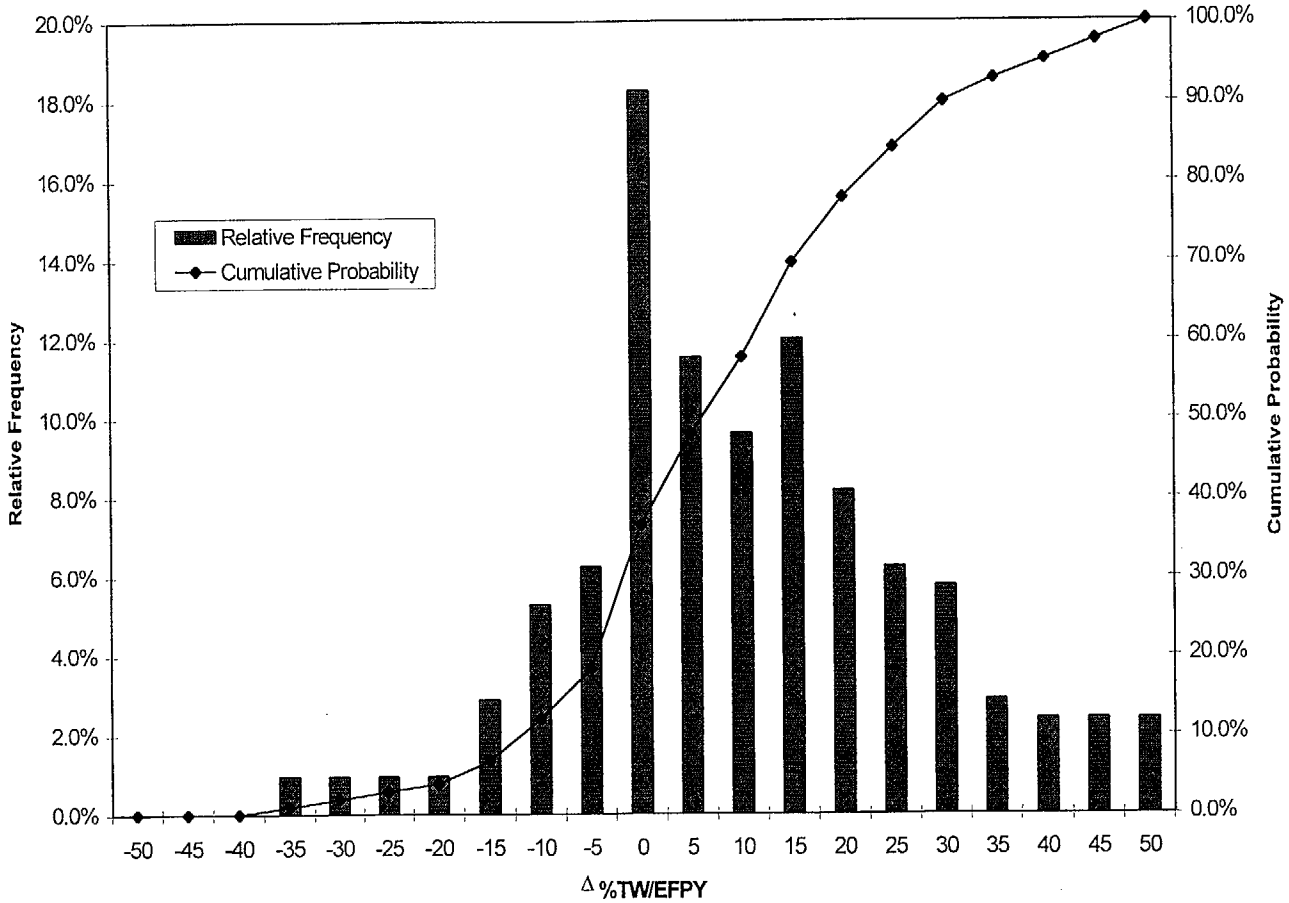

Figure 5-4 — Apparent ANO-2 Axial Flaw Growth Rate (2P99 – 2R13).

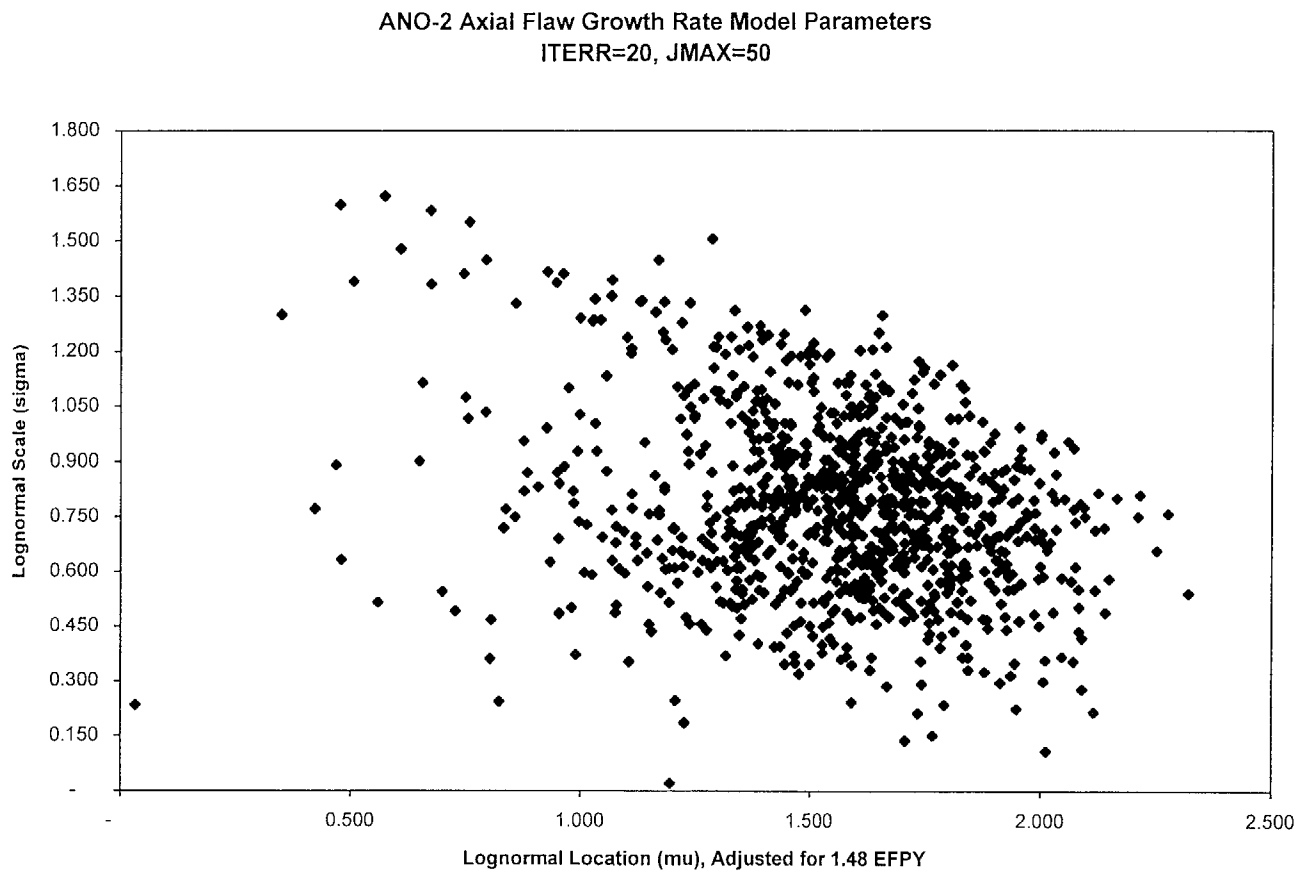

Figure 5-5 — ANO-2 Axial Flaw Actual Growth Model Parameters.

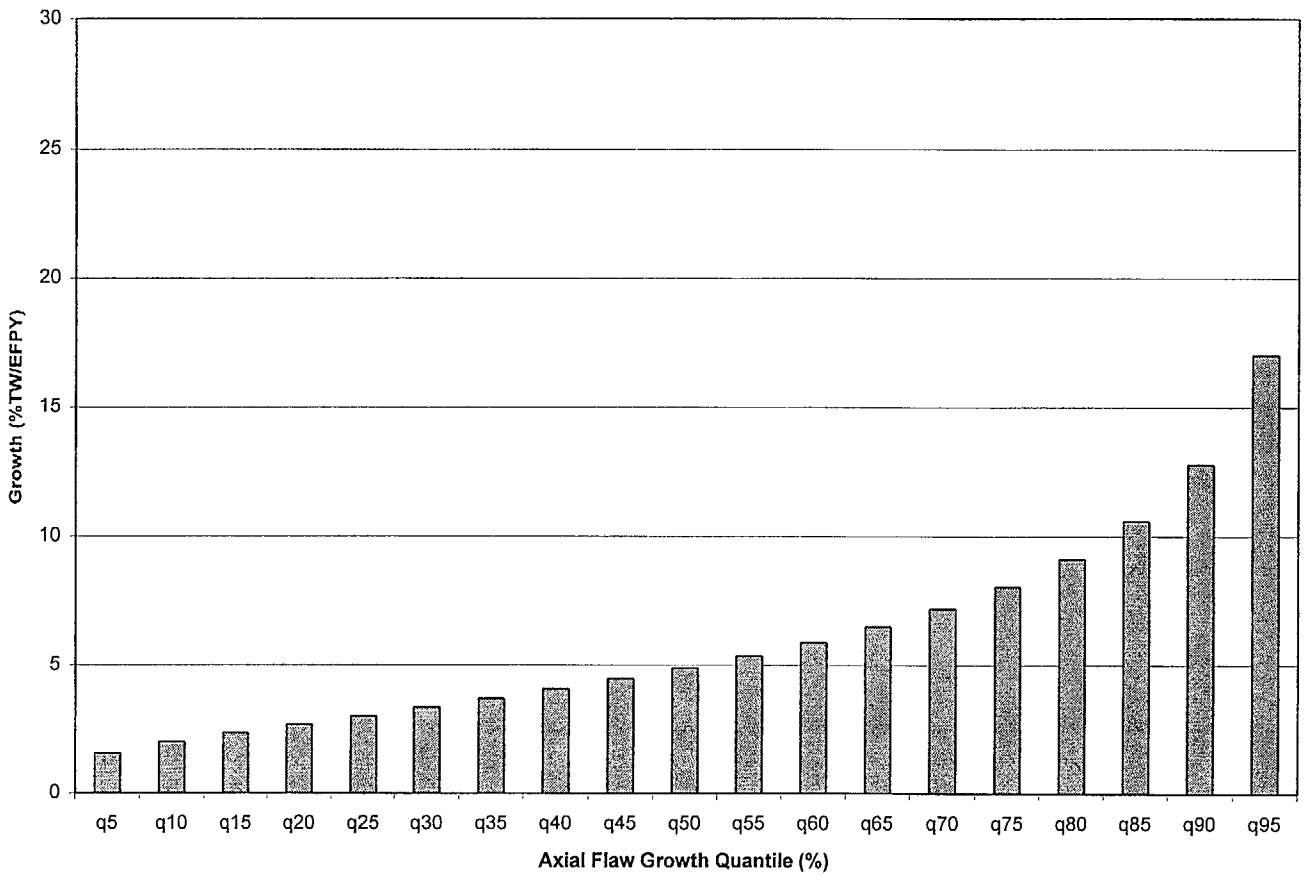

Figure 5-6 — Best-Estimate ANO-2 Axial Flaw Actual Growth Rates (Unadjusted).

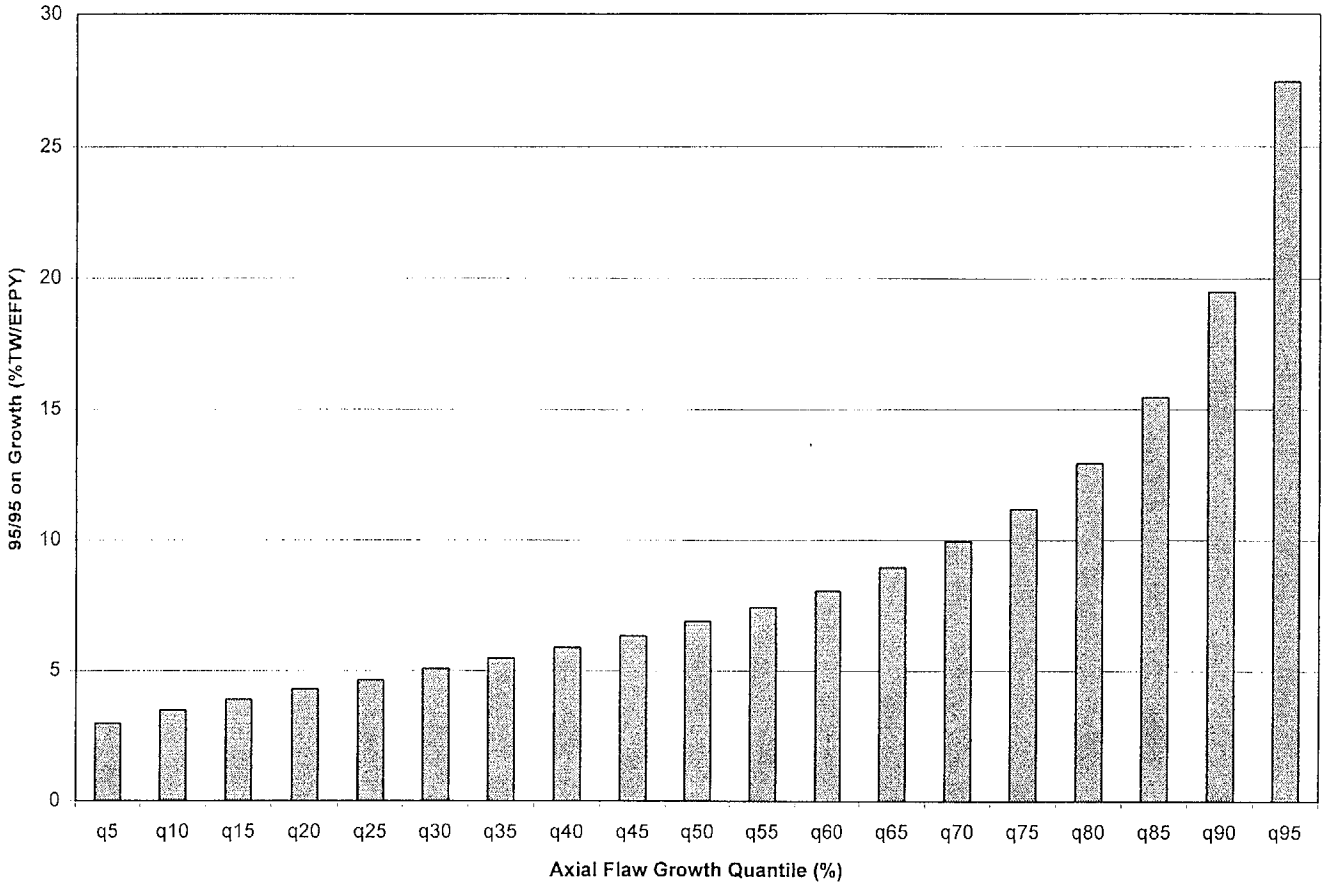

Figure 5-7 — 95/95 ANO-2 Axial Flaw Actual Growth Rates (Unadjusted).

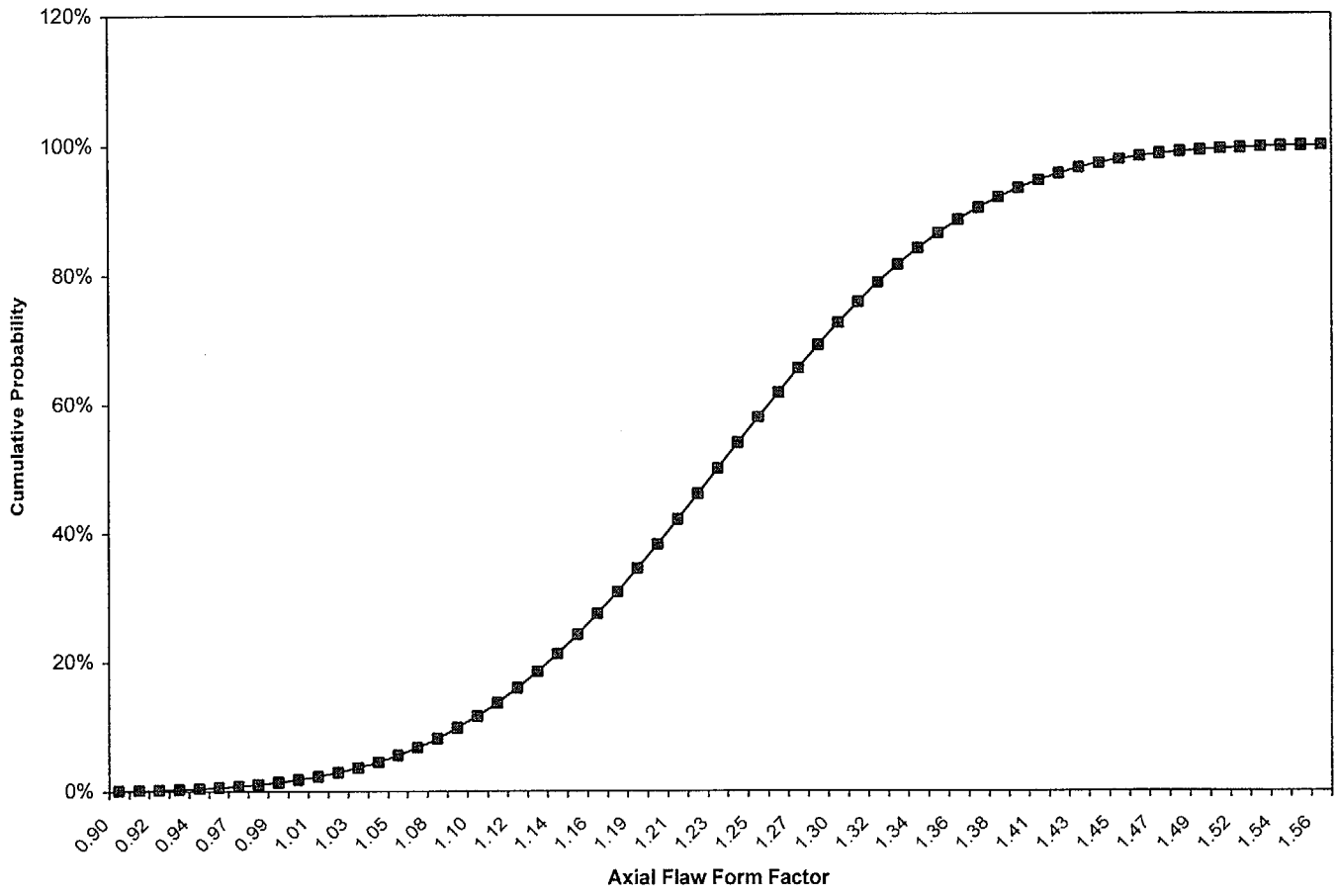

Figure 5-8 — ANO-2 Axial Flaw Form Factor Distribution.

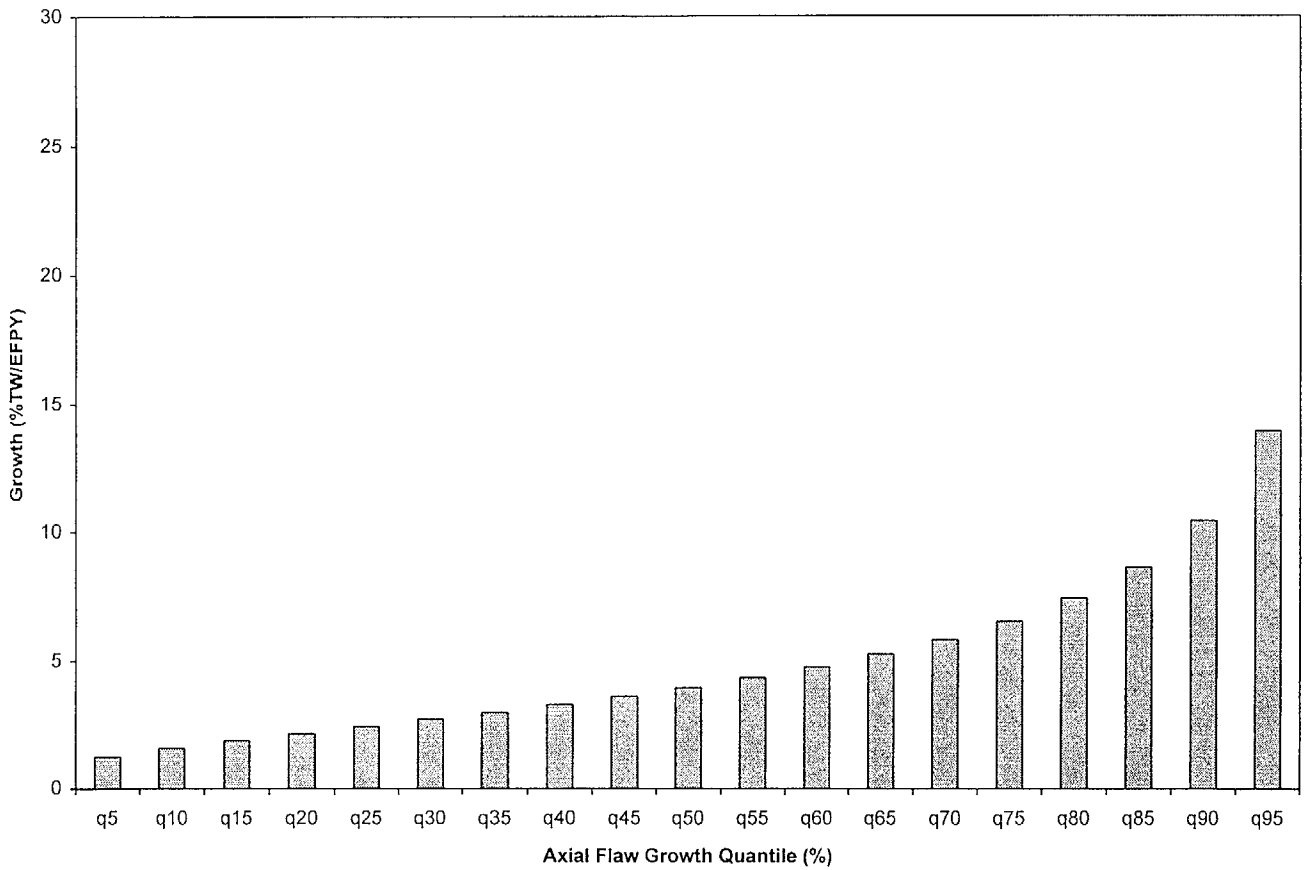

Figure 5-9 — Best-Estimate ANO-2 Axial Flaw Growth Rate (Adjusted).

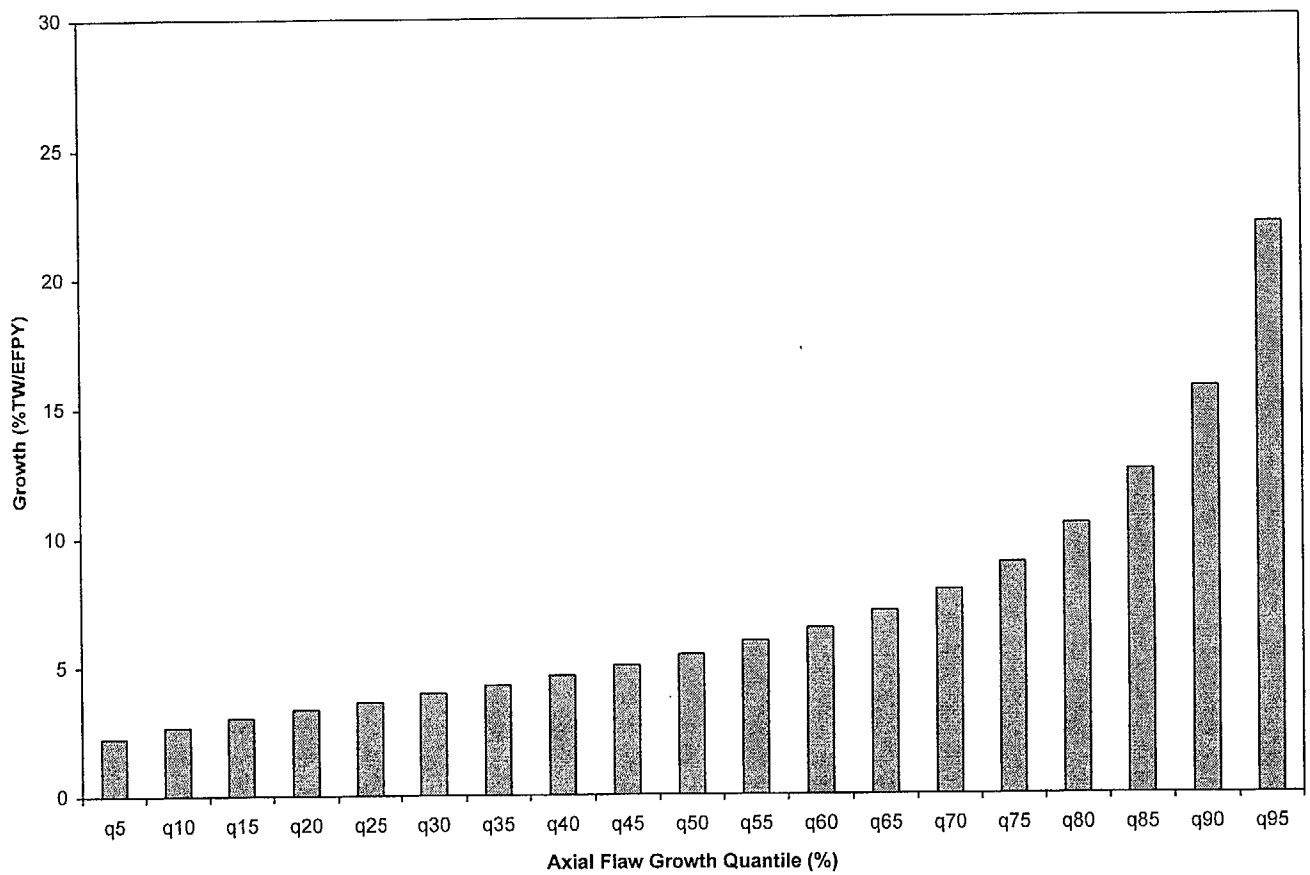

Figure 5-10 — 95% CL for ANO-2 Axial Flaw Growth (Adjusted).

Section 6

RESULTS: STRUCTURAL MARGIN AND LEAKAGE EVALUATIONS

A Monte Carlo simulation process was used to model the evolution of ODSCC degradation at eggcrate intersections in SG tubes at ANO-2. Complete emphasis was given to the modeling of the NDE process at the 2P99 SG inspection outage. A new single-cycle approach was used to incorporate only the most recent POD results reflecting current inspection capabilities. The primary figure of merit in this analysis was the POB at 3ΔP.

The POB at 3ΔP and corresponding leakage under SLB (13) accident conditions are given in Table 6-1 for the fully probabilistic burst pressure model. An additional case was run with the lower limit burst pressure model which predicted an EOC burst probability of approximately 20% at 0.85 EFPY. This corresponds closely with the burst probability cited in Ref. 14.

In addition to the standard assessment cases a parametric study was performed with the model to provide input for severe accident analyses. The results of this are shown in Table 6-2 which provides burst probabilities as a function of differential pressure and time-in-cycle. This analysis was performed with an earlier and more adverse 2P99 depth distribution.

Table 6-1

END OF CYCLE 14 RESULTS

Case	P (Burst) @ 3ΔP	P (Burst) @ SLB	Leakage @ SLB
Probabilistic Burst Model	0.049	0.00104	<0.01 gpm
Limit Burst Model	0.20	---	---

Table 6-2

PARAMETRIC STUDY RESULTS

EFPY / Δp	2500	3500	4050	5500	6000
14.96 (1)	0.0004	0.0088	0.0290	0.319	0.565
15.46 (1)	0.00097	0.0158	0.0499	0.462	0.726
15.81 (1)	0.00209	0.0288	0.0854	0.604	0.838
14.96 (2)	0.00227	0.0351	0.1057	0.755	0.946
15.46 (2)	0.00414	0.058	0.1735	0.884	0.985
15.81 (2)	0.00761	0.098	0.2659	0.947	0.995

Notes:

(1) Best-estimate burst model
(2) Lower limit burst model > 95/95

REFERENCES

1. Brown, S. D., "Detection Probability for Axial ODSCC at Support Structures Determined Using a Supplemental Performance Demonstration," Aptech Engineering Services, Inc., APTECH Report AES 99033642-1-2 (May 1999).

2. Sweeney, K., "Palo Verde Nuclear Generating Station Unit 2 SG Evaluation," Arizona Public Service Company Report (August 1995).

3. Begley, J. A., "Analysis of ODSCC/IGA at Tubesheet and Tube Support Locations at St. Lucie Unit 1," APTECH Report AES 96052749-1-1, Aptech Engineering Services, Inc. (October 1996).

4. Begley, J. A. and B. W. Woodman, "An Analysis of ODSCC/IGA at Eggcrate Support Locations at Arkansas Nuclear One (ANO) Unit 2," Aptech Engineering Services, Inc., APTECH Report AES 95102556-1-1 (March 1996).

5. "Palo Verde Nuclear Generating Station Unit 3 Cycle 6 SG Evaluation," Arizona Public Service Company, Submitted to the Nuclear Regulatory Commission (July 1996).

6. Woodman, B. W. and J. A. Begley, "Palo Verde Unit 2 Run Time Analysis Regarding the Impact of Upper Bundle corrosion Degradation During Cycle 7," Aptech Engineering Services, Inc., APTECH Report AES 96072812-1-1, Rev. 1 (December 1996).

7. Cochet, B., "Assessment of the Integrity of SG Tubes – Burst Test Results – Validation of Rupture Criteria (FRAMATOME DATA)," Palo Alto, CA, Electric Power Research Institute, EPRI NP-6865-L, Vol. 1 (June 1991).

8. Begley, C. J. and J. A. Begley, "A Generic Probabilistic Analysis of the Effect of Axial Freespan Corrosion on the Structural Performance and Leak Rate Behavior of OTSG Tubing," APTECH Report AES 96102886-1Q-1 Aptech Engineering Services, Inc. (June 1997).

9. "PICEP: Pipe Crack Evaluation Program (Revision 1)," Electric Power Research Institute, EPRI NP-3596-SR, Revision 1 (December 1987).

10. "Depth-Based Structured Analysis Methods for SG Circumferential Indications," Electric Power Research Institute, EPRI TR-107197-P1 (November 1997).

11. Begley, J. A., "Leak Rate Calculations for Axial Cracks in SG Tubing," Aptech Engineering Services, Inc. APTECH Calculation AES-C-2797-2 (April 1997).

12. "PWR SG Tube Repair Limits – Technical Support Document for Outside Diameter Stress Corrosion Cracking at Tube Support Plates," Electric Power Research Institute, EPRI Report TR-00407, Rev. 1 (August 1993).

13. "SLB Leak Rate and Tube Burst Probability Analysis Methods for ODSCC at TSP Intersections," Westinghouse Non-Proprietary Class 3 Report, WCAP 14277, Revision 1 (December 1996).

14. Enclosure 1 "Joseph M. Farley Nuclear Plant – Unit 1 Cycle Length Evaluation Analysis", Letter, D. Morey (Southern Co.) to Document Control Desk USNRC, NEL-99-0173, April 23, 1999

15. "APTECH Axial Crack Burst Pressure Methodology", Aptech Engineering Services, Inc. APTECH Report AES 96112906-1Q-2, August 1999, Revision 1.

Business Units:

- Fossil Power Services, Nuclear Power Services, Petrochemical Oil & Gas, Legal & Insurance Litigation, Industrial

Headquarters
1282 Reamwood Avenue, Sunnyvale, California 94089
Post Office Box 3440, Sunnyvale, California 94088-3440
Phone: 800.477.2228, Fax: 408.734.0445
Website: www.aptecheng.com

Offices
Houston, TX, 281.558.3200
Charlotte, NC, 704.865.6318
St. Louis, MO, 636.394.2653
Washington, DC, 301.868.4899

APTECH Engineering Services, Inc.

Attachment 6